Environ. Sci. Technol. **1998**, *32,* 1596−1603

Variation of Surface Charge Density in Monoclonal Bacterial Populations: Implications for Transport through Porous Media

J. C. BAYGENTS,* J. R. GLYNN, JR., O. ALBINGER, B. K. BIESEMEYER, K. L. OGDEN, AND R. G. ARNOLD

Department of Chemical and Environmental Engineering, The University of Arizona, Tucson, Arizona 85721

The forced convection of a monodisperse, monoclonal suspension of bacteria through a uniform, saturated porous medium has been investigated. Bench-scale column studies were carried out to measure the removal of microorganisms from suspension due to attachment to the surfaces of the solid phase. The columns were packed with 40-μm borosilicate glass beads, and bacterial sorption was measured as a function of depth in the column using a leucine radiolabel assay. The strains A1264 and CD1 were examined separately. Colloid filtration theory was used to interpret the data, and the average, or effective, affinity of the bacteria for the glass beads was found to decrease with distance traveled through the column. It is postulated that, under these circumstances, the cell/collector affinity (that is, the collision efficiency α) varied due to intrapopulational differences in bacterial surface characteristics. A simple bimodal probability density function, consisting of two Dirac delta functions, was found to satisfactorily represent the α distribution in the original bacterial population. This form of the distribution function was supported by capillary electrophoresis measurements on the bacteria, which showed intrapopulational differences in the surface charge density under the conditions of the transport experiments. These variations in surface charge density are significant inasmuch as they give rise to substantial differences in the colloidal interaction potentials and, presumably, large differences in cell affinity for negatively charged collectors such as glass beads or quartz.

Introduction

Bacterial transport in porous media is central to a variety of contemporary environmental issues, including filtration efficiency, pathogen transport in aquifers (*1*), in situ bioremediation of subsurface contaminants (*2*), oil field repressurization (*3*), and the origin of bacteria in deep subsurface sediments (*4*). Predictive descriptions of bacterial transport and removal associated with flow through porous media are commonly based on models that treat bacteria as discrete, colloidal particles. Attachment of such particles to the collectors that comprise the porous medium is seen as a two-step process: transport to the surface due to advection, sedimentation, Brownian diffusion, etc., followed by physical attachment to the surface (*5*). The second step is characterized by an efficiency parameter α (that is, the collision efficiency), which is defined as the fraction of particles retained after the collector surface is encountered (*6*).

Variation in α among bacterial species can be significant for a single collector material. For example, in our laboratory, 3 orders of magnitude variation in α have been observed among bacterial species screened for affinity to borosilicate glass (*7*). Such results imply that the concentrations of the species with the greatest and least affinity for the collector will be comparably attenuated from solution during passage over distances of 1 m and 1 km, respectively.

Albinger et al. (*8*) indicated that α values are distributed, even for collisions involving monoclonal bacterial populations and an ostensibly uniform collector surface. These α distributions were not attributable to intrastrain genetic or size variations. Explanations postulated for the heterogeneous collision efficiency included intrapopulation variations in metabolic activity (*9*) and electrical surface charge density (*10*). Here we examine this matter further, as we investigate the nature and source of the α distributions for two different bacterial species and present electrokinetic evidence that physicochemically significant differences in surface charge density exist within each of the populations. The ability of intrastrain surface charge variation to account for observed variation in α values is examined.

Inasmuch as there is no satisfactory theoretical basis for predicting the collision efficiencies of nonsticking (low α) particles during transport through porous media (*11, 12*), several methods have been devised for calculating α from colloid retention data (*13*−*15*), and this is the approach that we take here. In particular, Gross et al. (*15*) described procedures, which we refer to as the MARK (microbe and radiolabel kinesis) method, that lead to reproducible measurements of collision efficiency for $\alpha > 3 \times 10^{-5}$. The fraction of cells retained in short columns is then converted to an estimate of the population collision efficiency using the semiempirical method of Rajagopalan and Tien (*16*) and Rajagopalan et al. (*17*).

Using an extension of the general MARK procedure, Albinger et al. (*8*) divided the collector material into approximately millimeter-thick cross sections and found monotonic, order-of-magnitude decreases in $\bar{\alpha}$, the effective α value of the population, over glass bead columns that were only 1 cm in length. When such $\bar{\alpha}$ variation is attributable to heterogeneity among the organisms, predictive models of biocolloid transport/retention in porous media depend on a faithful representation of $f(\alpha)$, the probability density function (pdf) that describes the α distribution within the population. It is easy to envision pdf's that would include a finite number of microorganisms with extremely low probabilities of adhesion. Those cells could be transported over long distances—orders of magnitude further than would be predicted using filtration theory and a uniform, experimentally determined α value.

Here we evaluated a series of candidate multiparameter $f(\alpha)$ with regard to their respective abilities to account for biocolloid attenuation during advection-dominated transport of monoclonal bacterial populations through uniform porous media. The physiological basis of distributed α values was also investigated. Capillary electrophoresis measurements showed that each of the studied bacterial strains exhibited two substantial electrophoretic mobility modes, meaning

* Author to whom correspondence should be addressed. Present address: Department of Math and Statistics, the University of Melbourne, Parkville, VIC 3052, Australia [telephone: (520) 621-6044; fax: (520) 621-6048; e-mail: jcb@maxwell.che.arizona.edu].

S0013-936X(97)00711-6 CCC: $15.00
Published on Web 04/17/1998

that there are in fact intrapopulation variations in the surface charge density of the organisms.

Colloid Filtration Theory and the MARK Column Experiments

On the basis of the filtration theory of Yao et al. (*18*) and the semiempirical methods of Rajagopalan and Tien (*16*) and Rajagopalan et al. (*17*), transport of colloidal particles through saturated, isotropic porous media can be represented by a convective dispersion equation, augmented by adsorption and desorption terms to account for bacterial interaction with the collector surface (*5*). The MARK experiments outlined in the subsequent section are performed in cylindrical columns packed with 40-μm glass spheres that were initially free of bacteria. Accordingly, there was a large excess of clean surface to which the bacteria could attach. Over the course of the experiment, during which ≈10 pore volumes of the bacterial suspension passed through the columns, the local attachment rate was assumed to be linear in the bacterial concentration and detachment was neglected. Because the flows were strong, the mass balance on the microorganisms simplifies to

$$F(x) = 1 - [c(x)/c_0] = 1 - \exp(-N_{Da}\alpha x) \qquad (1)$$

where $F(x)$ is the fraction of influent bacteria retained between the inlet and x, the (dimensionless) axial position scaled on L, the length of the MARK column; c_0 is the influent concentration of bacteria; $c(x)$ is the concentration of bacteria in suspension; N_{Da} is a Damköhler number characterizing the rate of bacterial collisions with the collector relative to the rate of advective transport; and α is the efficiency of the collisions. For a uniform bed of spherical collectors, $N_{Da} \equiv 3(1-\theta)\eta L/2d_c$, where θ is the porosity of the bed and d_c is the diameter and η the collector efficiency of the individual beads. An empirical relationship was used for η in this work, as described by Logan et al. (*19*).

A straightforward rearrangement of eq 1 suggests that a plot of $\ln[1 - F(x)]$ versus x ought to vary linearly with a slope of $-N_{Da}\alpha$, that is

$$\ln[1 - F(x)] = -N_{Da}\alpha x \qquad (2)$$

However, the experiments of Albinger et al., as well as data to be described under Results and Discussion, strongly imply that α need not be uniform for the entire bacterial population. In such instances, eq 1 becomes

$$F(x) = 1 - \int_0^1 f(\alpha) \exp[-N_{Da}\alpha x]\, d\alpha \qquad (3)$$

if the collision efficiency is represented by a probability density function $f(\alpha)$, where $f(\alpha)\, d\alpha$ is the probability that a bacterium within the population will have a collision efficiency between those of α and $\alpha + d\alpha$.

In principle, measurements of bacterial retention as a function of depth can be used to deduce the form of $f(\alpha)$. In the section that follows, we describe such experiments on bacterial retention, which were performed on two separate strains. We extend previous work by (i) generating an internally consistent set of MARK (depth-dependent) column retention data for two subsurface bacterial isolates, (ii) using MARK data to deduce the mathematical form of $f(\alpha)$, and (iii) probing physiological explanations for apparent $f(\alpha)$ distributions. In that regard, capillary electrophoresis measurements enabled us to look directly for distributed electrophoretic mobilities in the same, ostensibly uniform populations of monoclonal, monodisperse bacteria.

Materials and Methods

The microbes used were A1264, a motile, ellipsoidal bacterium (l/w = 2.5) isolated from the Savannah River deep subsurface environment, and CD1, a nonmotile, ellipsoidal bacterium (l/w = 1.5) isolated from sediments at the Department of Energy site at Oyster, VA. The (Stokes–Einstein) radii of the bacteria, a_b, were 0.39 and 0.50 μm for A1264 and CD1, respectively, as measured with an N4 Plus particle size analyzer (Coulter, Inc.). Each strain was Gram-negative. Neither produced significant extracellular polysaccharides, as indicated by a ruthenium red dye adsorption method (*20*). Bacteria were grown to early stationary phase in 250-mL Erlenmeyer flasks containing 100 mL of 10% PTYG (0.25 g/L peptone, 0.25 g/L tryptone, 0.50 g/L yeast extract, 0.50 g/L glucose, 0.60 g/L $MgSO_4 \cdot 7H_2O$, and 0.07 g/L $CaCl_2 \cdot 2H_2O$) at room temperature (22–24 °C) on an orbit shaker table at 150 rpm.

MARK transport studies were conducted as described by Albinger et al. (*8*) with the following modifications. The experimental cultures were suspended in 3-[*N*-morpholino]-propanesulfonic (MOPS) buffer (4.186 g of MOPS acid/L, Sigma Ultra, titrated to pH 7.02 with 1 N NaOH, conductivity 760 μS/cm, ionic strength 10^{-2} M, filter sterilized) at a concentration of 10^6 cells/mL. The collector material consisted of 40-μm borosilicate glass beads (Whatman). Additional studies, to confirm the importance of electrostatic interactions, were performed by varying the ionic strength of the carrier solution from 10^{-2} to 1.0 M by the addition of KCl to the MOPS buffer. The collector material for those experiments was 38-μm soda-lime glass beads (Potters Industries, Inc.). In all of the experiments, the beads were pretreated as described by Gross et al. (*15*), and the bacterial suspension was passed through the column at $\approx 1.3 \times 10^{-1}$ cm/s.

The electrophoretic mobilities of the bacteria were measured with a Beckman P/ACE System 2100 capillary zone electrophoresis (CZE) unit using procedures that were described in detail by Glynn et al. (*21*). Experimental cultures were grown to early stationary phase under the conditions used for the MARK assays. Bacteria were resuspended at a final concentration of 10^9–10^{10} cells/mL and incubated at room temperature for 18 h. Stained cells were visually inspected to confirm that the suspensions were monodisperse. Culture purity was repeatedly verified by light microscopy and plating/colony morphology. The applied electric fields were typically 88–175 V/cm for measurements on CD1 and 319–426 V/cm for measurements on A1264. Higher voltage gradients were required for A1264 because, at low field strengths, significant peak broadening occurred; this was thought to be caused by microbial motility. A neutral marker, mesityl oxide, was introduced into the sample (2 μL of mesityl oxide into 400 μL of suspension) to indicate the velocity of the electroosmotic flow. Electrokinetic measurements were also performed on the background buffer (MOPS) and bacterial filtrate, which was obtained by passing the bacterial suspension through a 0.2-μm Acrodisc sterile filter.

Once the electrophoretic mobility M was established, the Smoluchowski equation (*12*) was used to determine the ζ potential of the bacteria

$$\zeta_b = \mu M/\epsilon\epsilon_0 \qquad (4)$$

where μ is the buffer viscosity, ϵ is the relative permittivity of the buffer, and ϵ_0 is the permittivity of the vacuum. Use of the Smoluchowski equation is valid provided that

$$e^{|z_{max}e\zeta_b/k_BT|}/\kappa a_b \ll 1 \qquad (5)$$

where κ is the Debye length, k_BT is the Boltzmann temperature, e is the fundamental charge on a proton, and z_{max} is the highest valence of the counterions in solution (*22*). The dimensionless Debye length $1/\kappa a_b$, for the bacteria suspended in aqueous MOPS buffer (ionic strength = 10^{-2} M) was

TABLE 1. Optimum Parameters from Fit of Empirical Probability Density Functions for $f(\alpha)$ to MARK Column Data

	bimodal distribution parameters[a]				Weibull distribution parameters[b]		
organism	f_{high}	α_{high}	α_{low}	R^2	A_w	B_w	R^2
A1264	0.17	0.83	1.00×10^{-2}	0.999	1.0×10^{-4}	0.27	0.841
CD1	0.02	1.15	3.30×10^{-3}	0.994	1.0×10^{-4}	0.07	0.889

[a] $f(\alpha) = (1 - f_{high})\delta(\alpha - \alpha_{low}) + f_{high}\delta(\alpha - \alpha_{high})$. [b] $f(\alpha) = A_w B_w \alpha^{B_w - 1} \exp(-A_w \alpha^{B_w})$.

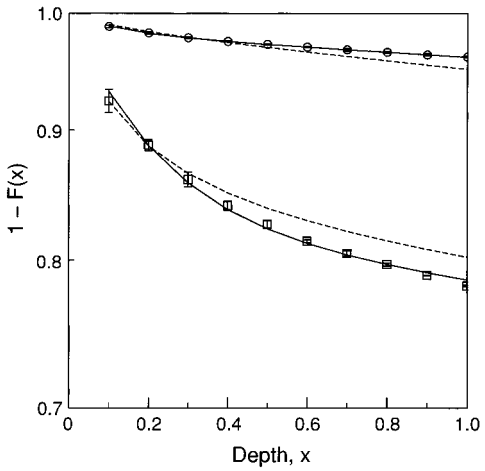

FIGURE 1. Comparison of MARK experiments on bacterial retention with eq 3. Data are shown as $\log_{10}[1 - F(x)]$ versus x for A1264 and CD1 on 40-μm borosilicate glass beads in 10^{-2} M MOPS buffer. Column length $L = 1$ cm. (□) MARK data for A1264; (○) MARK data for CD1; (– –) Weibull distribution; (—) bimodal distribution. Fitted parameters for the Weibull and bimodal distributions are found in Table 1.

approximately 1/165, $z_{max} = 1$, and $0.8 \leq e\zeta_b/k_BT \leq 1.5$ (based on the CZE results), so inequality (*5*) was satisfied.

The ζ potential of the borosilicate glass beads was measured using a Lazer Zee meter model 501 (Pen Kem, Inc.). The beads were pretreated as in the MARK procedure. Measurements were made in the same MOPS buffer as used for both the MARK transport and the capillary electrophoresis studies. The surface charge density of the soda-lime glass beads was available from literature (*23*).

Results and Discussion

MARK Column Studies. The results of MARK column experiments for the A1264 and CD1 strains are shown in Figure 1. The data are displayed as semilog plots of $1 - F(x)$ versus x, the depth in the column. Individual data points represent values averaged over three experiments, and the error bars are two standard deviations wide. According to standard clean-bed filtration theory, as represented by eq 2, $\log_{10}[1 - F(x)]$ should vary linearly with x. The nonlinear relationships obtained here are consistent with those reported by Albinger et al. (*8*).

Also shown in the figures are mathematical interpretations of the data based on eq 3. The dashed curve was generated by assuming that $f(\alpha)$, the pdf for α, is given by the two-parameter (A_w and B_w) Weibull distribution (*24*)

$$f(\alpha; A_w, B_w) = A_w B_w \alpha^{B_w - 1} \exp(-A_w \alpha^{B_w}) \quad \text{for } \alpha, A_w, B_w > 0 \quad (6)$$

The solid line was generated by taking $f(\alpha)$ to be a discrete, bimodal function of α

$$f(\alpha;\alpha_{low}, \alpha_{high}, f_{low}, f_{high}) = f_{low}\delta(\alpha - \alpha_{low}) + f_{high}\delta(\alpha - \alpha_{high})$$

$$\text{for } \alpha_{low}, \alpha_{high}, f_{low}, f_{high} > 0, \text{ with } f_{low} + f_{high} = 1 \quad (7)$$

where δ is the Dirac delta function, α_{low} and α_{high} are the collision efficiencies, and f_{low} and f_{high} are the fractions of the total population associated with each mode. The optimum values of the parameters A_w and B_w for the Weibull distribution, as well as the parameters α_{low}, α_{high}, and f_{high} for the discrete, bimodal distribution, appear in Table 1. These were established by optimizing the coefficient of determination R^2 (*25*), thereby minimizing the error between $F_{exp}(x_i)$, the experimentally measured fraction of influent bacteria retained between the inlet and position x_i ($i = 1, ..., 10$) in the column, and $F_{fit}(x_i)$ calculated from the right-hand side of eq 3 with the assumed distribution for $f(\alpha)$ (that is, eq 6 or 7) substituted into the integral. For the Weibull distribution, the integral was evaluated numerically with composite Newton–Cotes formulas (*26*).

The upper limit on the integral in eq 3 was allowed to go beyond unity since, for α to be strictly confined to values between 0 and 1, the calculation of the collector efficiency must be without flaw. Unfortunately, there are empirical uncertainties associated with the calculation of η (*12*), and α values >1 are often obtained (*27*, *28*). It should be noted, though, that substantially the same results were obtained when it was stipulated that $0 \leq \alpha \leq 1$.

In addition to the Weibull distribution, various other unimodal, two-parameter probability distribution functions were considered, including normal, log-normal, gamma, and inverse Gaussian. Of these, the Weibull distribution gave the best agreement with the data. It is clear from Figure 1, however, that the three-parameter bimodal distribution given by eq 7 provides a more faithful representation of the data.

Our rationale for investigating a bimodal $f(\alpha)$ stems from the observations that (1) according to eq 2, the effective α of the population in suspension is proportional to the slope of the $\log_{10}[1 - F(x)]$ versus x curve; (2) the data shown in the figures suggest that the effective α (or slope) diminishes monotonically (in magnitude) with depth; and (3) there are relatively linear regions on each of the curves shown (Figure 1), near the top and bottom of the column. Inasmuch as repeated examinations indicated that culture purity was maintained, the simplest postulate is that the bacterial population consisted of two subpopulations: one sticky, the other less so. The sticky subpopulation would be easily removed, giving a steep slope to the $\log_{10}[1 - F(x)]$ versus x curve at the shallower depths. As the sticky population is removed, the less sticky organisms comprise an ever-growing proportion of the bacteria remaining in suspension and, so, the slope diminishes with depth.

Direct experimental support for a bimodal $f(\alpha)$ is found in the results of the electrokinetic measurements (see below). The importance of electrostatics to cell retention on glass beads was certainly expected. Meinders et al. (*29*) and von Loosdrecht et al. (*30*) showed that, for organisms that are not hydrophobic, bacterial attachment to glass is strongly influenced by electrostatic interactions. Experiments illustrating the dependence of bacterial attachment to collector media on ionic strength are commonplace (*31*–*33*).

The importance of electrostatics to cell retention was supported in our experiments by the observed dependence

TABLE 2. Effective Collision Efficiency $\bar{\alpha}$ as a Function of Cell Identity and Ionic Strength in 1-cm MARK Columns[a]

	effective collision efficiency,[b] $\bar{\alpha}$		
organism	$I = 10^{-2}$ M	$I = 10^{-1}$ M	$I = 1$ M
A1264	3.6×10^{-2}	8.4×10^{-2}	3.8×10^{-1}
CD1	1.7×10^{-2}	2.7×10^{-2}	6.5×10^{-2}

[a] The collector material for these experiments was 38-μm soda-lime glass beads. [b] Ionic strength I was varied by addition of KCl to 10^{-2} M MOPS buffer (pH 7.02).

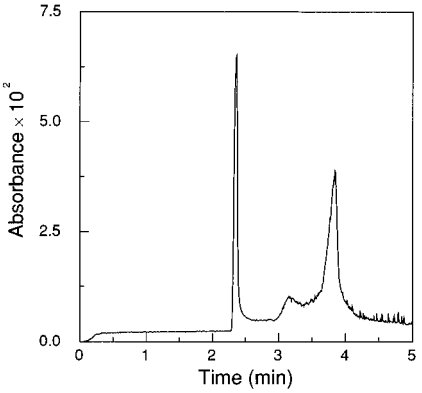

FIGURE 2. Typical electropherogram for A1264 showing elution times of the neutral marker (mesityl oxide elution time = 2.36 min) and two A1264 subpopulations (peak elution times = 3.16 and 3.85 min). UV absorbance was measured at $\lambda = 214$ nm. Measurements were conducted in 10^{-2} M MOPS buffer (pH 7.02) at 25 °C with an applied electric field strength of 426 V/cm over a 47-cm-long capillary.

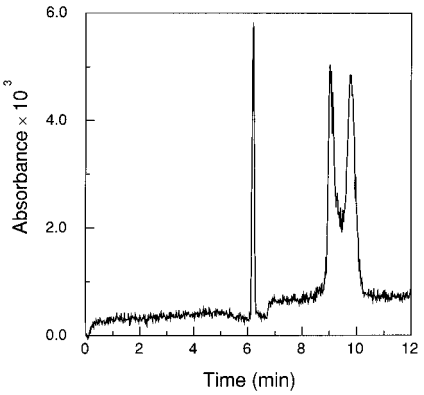

FIGURE 3. Typical electropherogram for CD1 showing elution times of the neutral marker (mesityl oxide elution time = 6.21 min) and two CD1 subpopulations (peak elution times = 9.03 and 9.81 min). UV absorbance was measured at $\lambda = 214$ nm. Measurements were conducted in 10^{-2} M MOPS buffer (pH 7.02) at 25 °C with an applied electric field strength of 175 V/cm over a 57-cm-long capillary.

of $\bar{\alpha}$ (the effective collision efficiency over the length of 1-cm MARK reactors) on the ionic strength of the carrier solution. Increasing the ionic strength from 10^{-2} to 1.0 M by KCl addition caused a 10-fold increase in $\bar{\alpha}$ for A1264 and a 4-fold increase in $\bar{\alpha}$ for CD1 (Table 2). Furthermore, since bimodality in the electrophoretic behavior of microorganisms has been observed in several other contexts (*34*–*36*), intrastrain variation in cell surface charge provided a plausible candidate explanation for the depth-dependent α values observed in MARK column studies.

Electrophoresis Measurement. In Figures 2 and 3, typical electropherograms are shown for A1264 and CD1, respectively. The data for both A1264 and CD1 exhibited two strong modes (the first large peak in the figures is due to the neutral marker, mesityl oxide). The neutral marker had no detectable effect on the electrophoretic mobility of the microorganisms. The peak sizes suggest a large percentage contribution by each subpopulation; if a bacterial contaminant had been responsible for one of the peaks, it should have been visually observable. Moreover, neither the electrokinetic measurements on the buffer nor those on the filtrate yielded any peaks.

TABLE 3. Electrokinetic Data for A1264 and CD1

	A1264[a]	CD1[b]
M_1 (μm cm s^{-1} V^{-1})	-1.48 ± 0.16	-2.25 ± 0.11
M_2 (μm cm s^{-1} V^{-1})	-2.31 ± 0.12	-2.62 ± 0.15
ζ_1 (mV)	-20.87 ± 2.21	-31.72 ± 1.53
ζ_2 (mV)	-32.57 ± 1.73	-36.94 ± 2.11
% total peak area, 1st peak	28.9 ± 17.4	48.2 ± 15.2

[a] The means and standard deviations of results are based on 7 CE experiments; see Figure 2 for a typical result. [b] The means and standard deviations of results are based on 18 CZE experiments; see Figure 3 for a typical result.

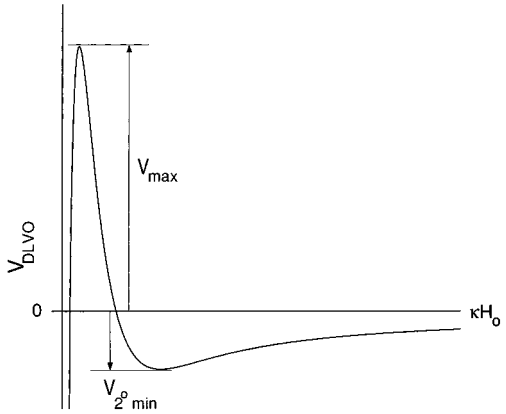

FIGURE 4. Qualitative features of the classical DLVO interaction energy V_{DLVO} as a function of dimensionless surface-to-surface separation H_0. The primary energy barrier V_{max} and the secondary minimum $V_{2^\circ\ min}$ are indicated in the figure.

Data from the A1264 and CD1 electropherograms were converted into ζ potentials for the bacteria with eq 4. The results of these calculations are summarized in Table 3 for the two electropherogram modes exhibited by each strain. In the table, and the text below, the subscripts 1 and 2 refer to the first and second bacterial peaks to emerge in the electropherograms. Note that, in the capillary electrophoresis experiments, the electroosmotic velocity of the carrier buffer is antiparallel to the electrophoretic velocity of the bacteria. Thus, the more highly charged bacteria are eluted last. The results clearly show that surface charge density can be a distributed function among stationary phase bacteria in pure cultures. For A1264, the difference in the ζ potentials associated with the mobility modes is $\Delta\zeta = \zeta_2 - \zeta_1 = -11.70 \pm 2.09$ mV. For CD1, $\Delta\zeta = -5.22 \pm 1.75$ mV. The ζ potential of the borosilicate glass beads, as determined with the Lazer Zee meter (Pen Kem, Inc.), was -37.58 ± 4.95 mV in 10^{-2} M MOPS buffer at pH 7.02.

Collision Efficiency Calculations Based on Electrophoresis Measurements. The Derjaguin–Landau–Verwey–Overbeek (DLVO) energy of interaction (V_{DLVO}) between a negatively charged colloid and a neighboring collector is obtained by combining London–van der Waals and electrostatic energies. When plotted as a function of separation distance H_0 (Figure 4), V_{DLVO} exhibits a deep primary minimum, an energy barrier V_{max} and a shallow secondary minimum $V_{2^\circ\ min}$.

TABLE 4. Summary of Approaches for the Prediction of Collision Efficiency from Physicochemical Parameters[a]

1. primary minimum capture[b] (*23*, *37*−*44*)
$$\alpha = 4A_s^{1/3}N_{Pe}^{-2/3}\eta^{-1}\beta(1+\beta)^{-1}S(\beta)$$
$$\beta = \frac{\sqrt[3]{4}}{3}\Gamma\left(\frac{1}{3}\right)A_s^{-1/3}N_{Pe}^{-1/3}(a_c K_F/D_P)$$
$$K_F = D_P\left(\int_0^{\delta_F}\{g_1(H_0)\exp[V_{DLVO}(H_0)/k_BT] - 1\}dH_0\right)^{-1}$$

2. secondary minimum capture (*11*)
$$\alpha = 1 - \exp(-|V_{2^\circ\ min}/k_BT|)$$

3. empirical correlation (*45*)
$$\log_{10}\alpha = \log_{10}B + n\log_{10}(\kappa A/\epsilon\epsilon_0\zeta_b\zeta_c)$$

[a] Notation is as defined under Nomenclature. V_{DLVO}, V_{max}, and $V_{2^\circ\ min}$ are as illustrated if Figure 4. [b] $S(\beta)$ was tabulated by Spielman and Friedlander (*38*). When $V_{max}/k_BT \gg 1$, this approach yields $\alpha \doteq \gamma \exp(-|V_{max}/k_BT|)$.

A variety of approaches have been developed to connect the collision efficiency α to the thermal and DLVO forces that presumably dominate the particle transport close to the collector surface; we have applied the three summarized in Table 4 to the analysis of our data.

The first approach has received widespread application and treats particle removal from suspension as a surface reaction in which the particles traverse the energy barrier V_{max} and are captured in the primary minimum. The reaction rate constant K_F accounts for the DLVO interactions, which influence particle transport within a boundary layer of thickness δ_F at the collector surface (*23*, *37*−*44*).

The second approach is heuristic and applies when the primary energy barrier precludes access of suspended particles to the collector surface. In these cases capture can still occur in the secondary energy minimum. Proceeding with the analogue of particle capture as a surface reaction, Hahn (*11*) has related α to the energy required to escape from the secondary minimum, that is, $V_{2^\circ\ min}$. This relationship is given in Table 4 and has been used to explain the colloid retention data of Elimelech and O'Melia, where analysis based on capture in the primary minimum failed (*23*, *44*).

The third approach that we employ is empirical and was put forth by Elimelech (*45*) to circumvent the difficulties in calculating α directly from first principles. Instead of relating α to V_{DLVO}, the collision efficiency is correlated with the primary DLVO interaction parameters, namely, the Hamaker constant (*A*), the Debye screening length, the dielectric constant of the solvent, and the ζ potentials of the interacting surfaces.

The results of the calculation of the collision efficiency by the three aforementioned approaches are summarized in Table 5 and are discussed below.

Comparison of MARK and Electrophoresis Measurements with Colloid Capture Theory. The empirical results and theoretical tools described to this point invite several comparisons. For example, it is possible to compare fitted f_{high} and f_{low} values (compare eq 7) with corresponding (relative) peak areas in the electropherograms. MARK data/curve fitting (Figure 1) indicated that f_{high} was ∼0.17 (Table 1), corresponding roughly to the relative area of the first peak in A1264 electropherograms (0.29 ± 0.174; Table 3). Electropherogram peak areas may, therefore, correspond to sticky and nonsticky subpopulations that are also manifested in MARK data. On the other hand, MARK data/curve fitting for strain CD1 indicated that $f_{high} < 0.02$ (Figure 1; Table 1), a value that is not easily reconciled with CD1 electropherograms (Table 3) in which the relative area of the first peak was 0.48 ± 0.152. Values of ζ_2 for A1264 (the nonsticky mode) and ζ_1 for the CD1 culture (Table 3) are similar; if the ζ potential is a primary determinant of sticking efficiency, the subpopulations contributing to the two primary peaks in the CD1 electropherogram (Figure 3) may both be comprised bacteria with relatively low α values. In the measurement of electrophoretic mobility by capillary electrophoresis, only ∼25 000 cells were injected, of which the sticky fraction (α = 1.15; Table 1) consisted of fewer than 500. The corresponding peak area, which should have been only 4% of those shown (Figure 3), would have been lost in baseline noise. Consequently, both of the major peaks in the CD1 electropherogram may correspond to low-affinity subpopulations, while the sticky fraction that produces declining α values lies below the detection limit of the CE device.

ζ potentials for both bacteria are sufficiently negative to prevent attachment within the primary energy minimum. That is, on the basis of the premise of capture in the primary minimum, calculated α values are vanishingly small, and, although corresponding α calculations remain sensitive to both ζ and *A*, differences are irrelevant in any practical sense. Calculated α values based on capture within the secondary minimum, while finite and reasonably sensitive to selection of *A*, are essentially independent of ζ potential in the range of those encountered here, $-36.96 \le \zeta \le -20.87$ mV. There are apparently irreconcilable differences between α values based on MARK measurements and theoretical predictions based on electrophoresis data and capture in either the primary or secondary minimum.

Applying Elimelech's empirical approach to calculate *n* (Table 5) leads to values of 10 for A1264 and 37 for CD1. Neither result is appealing on the basis of theoretical arguments, nor do they compare favorably with *n* values deduced by Elimelech (*45*), which were near unity for the attachment of various-sized polystyrene spheres to glass-bead collectors.

Thus, although variation in intrapopulation surface charge density was plainly evident using capillary electrophoresis, extant methods for calculating α fail to provide an adequate quantitative explanation for the distribution of α values that was deduced from the MARK data originating from the same bacteria. The apparent discrepancy between experiment and

TABLE 5. Comparison of Collision Efficiencies Calculated from Physicochemical Parameters with Collision Efficiencies Interpreted from MARK Data[a]

	A1264		CD1	
method of determination	α_{high}	α_{low}	α_{high}	α_{low}
MARK data[b]	0.83	1.00×10^{-2}	1.15	3.30×10^{-3}
primary min capture[c]	$<10^{-96}$	$<10^{-198}$	$<10^{-253}$	$<10^{-299}$
secondary capture[c,d]	0.16−0.98	0.16−0.97	0.19−0.99	0.19−0.99
correlation	$\log_{10}(\alpha_{high}/\alpha_{low}) = 0.20n$		$\log_{10}(\alpha_{high}/\alpha_{low}) = 0.07n$	

[a] The bases for predicting α from physicochemical parameters are summarized in Table 4. [b] Collision efficiencies determined from bimodal α distribution fit to MARK data, as summarized in Table 1. [c] The heterocoagulation model of Hogg et al. (*83*) was used to calculate the DLVO interaction energies. To obtain α_{high}, ζ_b was set equal to ζ_1 from Table 3; similarly, α_{low} was obtained by setting ζ_b equal to ζ_2. [d] The range of α values quoted are for Hamaker constants that span those reported for bacteria and glass (*84*), that is, $A = 4 \times 10^{-22}$ to 6×10^{-21} J.

theory is not confined to this study. Incorporation of DLVO theory into descriptions of particle capture have been largely unsuccessful when electrostatic repulsion is present (*12*, *23*, *44*−*53*). Efforts to overcome these shortcomings, while numerous, have been only partially successful. Agreement was achieved, for example, after development of a Gaussian pdf to represent the distribution of ζ potentials among colloidal particles (*46*, *49*). However, the coefficient of variation for distributed ζ potentials that was required to fit the data was often higher than 0.3. Taken together, the body of experimental evidence indicates that DLVO theory underestimates deposition or aggregation in conditions of strongly repulsive electrostatic interactions.

Recently, techniques have been developed that make the measurement of the forces acting between colloidal particles and surfaces possible (*54*). These measurements have illuminated the presence of short-range hydrophobic forces (*55*−*57*). These forces tend to be attractive when the surfaces are hydrophobic. Extension of classical DLVO theory to account for these forces (*58*) has been used to describe interactions between glycolipid bilayers (*57*) and to describe bacterial adhesion onto various surfaces (*29*, *59*, *60*). Use of DLVO extensions to describe bacterial adhesion has yielded mixed results (*29*), especially when the surfaces and organisms are not particularly hydrophobic—exactly the situation we are describing in this study.

It should be noted in closing that Hunter (*22*) and Israelachvili (*61*) reviewed numerous systems in which classical DLVO theory provides good agreement with experiment. DLVO theory has been sucessfully used to predict soap film thickness (*62*−*64*); swelling of clays (*22*); double-layer forces in various electrolytes between mica (*65*−*68*), sapphire crystals (*69*), silica (*70*), surfactants, and lipid bilayers (*71*−*74*); and double-layer forces in nonaqueous liquids (*75*, *76*). Furthermore, several authors have been able to qualitatively describe bacterial adhesion or aggregation using DLVO theory (*33*, *77*−*81*) or to correlate attachment and detachment with the energy well associated with the secondary minimum (*29*). These successes notwithstanding, incorporation of the basic theory (*12*, *23*, *44*−*53*) or extensions thereof [for example, extended DLVO (*58*)] into calculation of colloidal filtration, deposition, or stability remains an area for continued investigation.

To summarize, then, the contributions and shortcomings of work described herein are as follows:

1. For the cases presented here, electrostatics were a primary determinant of cell/collector affinity. Intrastrain variation in bacterial surface charge density, which was detected by CZE measurements, was probably responsible for observed variation in cell stickiness. As far as we know, this is the first use of capillary electrophoresis to establish the electrostatic origin of transport variants in pure bacterial suspensions.

2. Collision efficiencies determined by (a) transport experiments and (b) DLVO-based analysis of electrophoretic data cannot be reconciled.

Nomenclature

Italic Symbols

a_b, a_c	radius of bacteria and collector, respectively, m
A	Hamaker constant, J
A_s	geometric correction factor to account for neighboring collector particles, $2(1-p^5)/(2-3p+3p^5-2p^6)$
A_w, B_w	Weibull distribution parameters
B	preexponential factor from Elimelech correlation (*45*), cf. Table 4
c	concentration of bacteria in suspension, m^{-3}
c_0	inlet concentration of bacteria, m^{-3}
d_c	collector diameter, m
D_p	particle dispersivity, m^2/s
e	fundamental charge on a proton, 1.6×10^{-19} C
$f(\alpha)$	probability density function for α distribution of bacterial population
f_{high}, f_{low}	fraction of bacteria with collision efficiency α equal to α_{high} and α_{low}, respectively
$F(x)$	fraction of influent bacteria retained between the inlet and position x
$g_1(H_0)$	hydrodynamic resistance function (*39*)
H_0	surface-to-surface separation between bacterium and collector, m
k_B	Boltzmann's constant, J/K
K_F	psuedo-first-order rate constant for deposition in the primary minimum, m/s
L	length of MARK column, m
M	electrophoretic mobility, $m^2/v\cdot s$
n	exponential factor from Elimelech correlation (*45*), cf. Table 4
N_{Da}	Damköhler number, $3(1-\theta)\eta L/2d_c$
N_{Pe}	Peclet number, $2U_a a_c/D_p$
p	$(1-\theta)^{1/3}$
R^2	coefficient of determination
$S(\beta)$	slowly varying function tabulated in ref 38, varies between 1.0 and 1.4
T	absolute temperature, K
U_a	approach velocity of the fluid, m/s
$V_{2^\circ\ min}$	DLVO potential energy of the secondary minimum, J
V_{DLVO}	total (van der Waals + electrostatic) DLVO interaction energy, J
V_{max}	DLVO potential energy barrier, J
x	dimensionless axial position in the MARK column
z_{max}	highest valence of counterions in solution

Greek Symbols

α	collision efficiency
β	colloidal interaction parameter, cf. Table 4
δ	Dirac delta function
δ_F	thickness of colloidal force boundary layer, cf. Table 4, m
γ	preexponential factor
Γ	the gamma function (*82*)
ϵ	relative permittivity of the buffer
ϵ_0	permittivity of free space, 8.854×10^{-12} C/V·m
η	collector removal efficiency
κ	Debye screening parameter, m^{-1}
θ	porosity of porous medium

ζ_b, ζ_c zeta potentials of bacterium and collector, respectively, V

Acknowledgments

We acknowledge the following gentlemen: Mr. Wallace Clark of the Division of Biotechnology, Arizona Research Laboratories, for his assistance with the capillary electrophoresis instrument; Dr. David Balkwill of Florida State University for providing the A1264 bacterial species; and Dr. Anthony Palumbo of Oak Ridge National Laboratory for providing CD1. This work was supported in part by Grant DE-FG03-94ER61887 from the Department of Energy Subsurface Science Program.

Literature Cited

(1) Keswick, B. H. In *Groundwater Pollution Microbiology*; Bitton, G., Gerba, C. P., Eds.; Wiley: New York, 1984; pp 39−64.
(2) Gerba, C. P. In *Groundwater Quality*; Ward, C. H., Giger, W., McCarty, P. L., Eds.; Wiley: New York, 1985; pp 53−67.
(3) Jang, L.-K.; Chang, P. W.; Findley, J. E.; Yen, T. F. *Appl. Environ. Microbiol.* **1983**, *46*, 1066.
(4) Balkwill, D. L. *Geomicrobiol. J.* **1989**, *7*, 33.
(5) Harvey, R. W.; Garabedian, S. P. *Environ. Sci. Technol.* **1991**, *25*, 178.
(6) Tien, C. *Granular Filtration of Aerosols and Hydrosols*; Butterworth Publishers: Stoneham, MA, 1989.
(7) Gross, M. J.; Logan, B. E. *Appl. Environ. Microbiol.* **1995**, *61*, 1750.
(8) Albinger, O.; Biesemeyer, B. K.; Arnold, R. G.; Logan, B. E. *FEMS Microbiol. Lett.* **1994**, *124*, 321.
(9) Kell, D. B.; Ryder, H. M.; Kaprelyants, A. S.; Westerhoff, H. V. *Antonie van Leeuwenhoek* **1991**, *60*, 145.
(10) Cowan, M. M.; van der Mei, H. C.; Rouxhet, P. G.; Busscher, H. J. *J. Gen. Microbiol.* **1992**, *138*, 2707.
(11) Hahn, M. W. Ph.D. Dissertation, Johns Hopkins University, Baltimore, MD, 1995.
(12) Russel, W. B.; Saville, D. A.; Schowalter, W. R. *Colloidal Dispersions*; Cambridge University Press: New York, 1989.
(13) Martin, R. E.; Bouwer, E. J.; Hanna, L. M. *Environ. Sci. Technol.* **1992**, *26*, 1053.
(14) Logan, B. E.; Hilbert, T. A.; Arnold, R. G. *Water Res.* **1993**, *27*, 955.
(15) Gross, M. J.; Albinger, O.; Jewett, D. G.; Logan, B. E.; Bales, R. C.; Arnold, R. G. *Water Res.* **1995**, *29*, 1151.
(16) Rajagopalan, R.; Tien, C. *AIChE J.* **1976**, *22*, 523.
(17) Rajagopalan, R.; Tien, C.; Pfeffer, R.; Tardos, G. *AIChE J.* **1982**, *28*, 871.
(18) Yao, K. M.; Habibian, M. T.; O'Melia, C. R. *Environ. Sci. Technol.* **1971**, *5*, 1105.
(19) Logan, B. E.; Jewett, D. G.; Arnold, R. G.; Bouwer, E. J.; O'Melia, C. R. *J. Environ. Eng.* **1995**, *121*, 869.
(20) Figueroa, L. A.; Silverstein, J. A. *Biotechnol. Bioeng.* **1989**, *33*, 941.
(21) Glynn Jr., J. R.; Belongia, B. M.; Arnold, R. G.; Ogden, K. L.; Baygents, J. C. *Appl. Environ. Microbiol.* **1998**, submitted for publication
(22) Hunter, R. J. *Introduction to Modern Colloid Sciences*; Oxford University Press: New York, 1993.
(23) Elimelech, M.; O'Melia, C. R. *Langmuir* **1990**, *6*, 1153.
(24) Miller, I.; Fruend, J. *Probability and Statistics for Engineers*; Prentice Hall: Englewood Cliffs, NJ, 1977.
(25) Hoerl, A. E. In *Perry's Chemical Engineers' Handbook*, Perry, R. H., Green, D. W., Maloney, J. O., Eds.; McGraw-Hill Book: San Francisco, CA, 1984; pp 2-109−2-113.
(26) Carnahan, B.; Luther, H. A.; Wilkes, J. O. *Applied Numerical Methods*; Wiley: New York, 1969.
(27) Johnson, W. P.; Martin, M. J.; Gross, M. J.; Logan, B. E. *Colloids Surf. A* **1996**, *107*, 263.
(28) Martin, M. J.; Logan, B. E.; Johnson, W. P.; Jewett, D. G.; Arnold, R. G. *J. Environ. Eng.* **1996**, *122*, 407.
(29) Meinders, J. M.; van der Mei, H. C.; Busscher, H. J. *J. Colloid Interface Sci.* **1995**, *176*, 329.
(30) van Loosdrecht, M. C. M.; Norde, W.; Lyklema, J.; Zehnder, J. B. *Aquat. Sci.* **1990**, *52*, 103.
(31) Seaman, J. C.; Bertsch, P. M.; Miller, W. P. *Environ. Sci. Technol.* **1995**, *29*, 1808.
(32) Mills, A. L.; Herman, J. S.; Hornberger, G. M.; DeJesús, T. H. *Appl. Environ. Microbiol.* **1994**, *60*, 3300.
(33) Zita, A.; Hermansson, M. *Appl. Environ. Microbiol.* **1994**, *60*, 3041.
(34) Cowan, M. M.; van der Mei, H. C.; Stokroos, I.; Busscher, H. J. *J. Dent. Res.* **1992**, *71*, 1803.
(35) Eisen, A.; Reid, G. *Microb. Ecol.* **1989**, *17*, 17.
(36) Bauer, J. In *Cell Electrophoresis*; Bauer, J., Ed.; CRC Press: Boca Raton, FL, 1994; pp 267−280.
(37) Ruckenstein, E.; Prieve, D. C. *J. Chem. Soc., Faraday Trans. 2* **1973**, *69*, 1522.
(38) Spielman, L. A.; Friedlander, S. K. *J. Colloid Interface Sci.* **1974**, *46*, 22.
(39) Dahnke, B. *J. Colloid Interface Sci.* **1974**, *48*, 520.
(40) Dahnke, B. *J. Colloid Interface Sci.* **1975**, *50*, 89.
(41) Dahnke, B. *J. Colloid Interface Sci.* **1975**, *50*, 194.
(42) Shapiro, M.; Brenner, H.; Guell, D. C. *J. Colloid Interface Sci.* **1990**, *136*, 552.
(43) Prieve, D. C.; Ruckenstein, E. *J. Colloid Interface Sci.* **1976**, *57*, 547.
(44) Elimelech, M.; O'Melia, C. R. *Environ. Sci. Technol.* **1990**, *24*, 1528.
(45) Elimelech, M. *Water Res.* **1992**, *26*, 1.
(46) Kihira, H.; Ryde, N.; Matijevic, E. *J. Chem. Soc., Faraday Trans.* **1992**, *88*, 2379.
(47) Marshall, J. K.; Kitchener, J. A. *J. Colloid Interface Sci.* **1966**, *22*, 342.
(48) Fitzpatrick, J. A.; Spielman, L. A. *J. Colloid Interface Sci.* **1973**, *43*, 350.
(49) Kihira, H.; Matijevic, E. *Langmuir* **1992**, *8*, 2855.
(50) Bleier, A.; Matijivic, E. *J. Colloid Interface Sci.* **1976**, *55*, 510.
(51) Sasaki, H.; Matijevic, E.; Barouch, E. *J. Colloid Interface Sci.* **1980**, *76*, 319.
(52) Hansen, F. K.; Matijevic, E. J. *Chem. Soc., Faraday 1* **1980**, *76*, 1240.
(53) Ottewill, R. H.; Shaw, J. N. *Discuss. Faraday Soc.* **1966**, *42*, 154.
(54) Claesson, P. M.; Ederth, T.; Bergeron, V.; Rutland, M. W. *Adv. Colloid Interface Sci.* **1996**, *67*, 119.
(55) Parker, J. L.; Claesson, P. M. *Langmuir* **1994**, *10*, 635.
(56) Yoon, R. H.; Flinn, D. H.; Rabinovich, Y. I. *J. Colloid Interface Sci.* **1997**, *185*, 363.
(57) Wood, J.; Luckham, P.; Swart, R. *Colloids Surf. A* **1993**, *77*, 179.
(58) van Oss, C. J. *Interfacial Forces in Aqueous Media*; Marcel Dekker: New York, 1994.
(59) Absolom, D. R.; Lamberti, F. V.; Policova, Z.; Zingg, W.; van Oss, C. J.; Neumann, A. W. *Appl. Environ. Microbiol.* **1983**, *46*, 90.
(60) Škvarla, J. *J. Chem. Soc., Faraday Trans.* **1993**, *89*, 2913.
(61) Israelachvili, J. N. *Intermolecular and Surface Forces*; Academic Press: San Diego, 1992.
(62) Derjaguin, B. V.; Titijevskaia, A. S.; Abricossova, I. I.; Malkina, A. D. *Discuss. Faraday Soc.* **1954**, *18*, 24.
(63) Lyklema, J.; Mysels, K. J. *J. Am. Chem. Soc.* **1965**, *87*, 2539.
(64) Donners, W. A. B.; Rijnbout, J. B.; Vrij, A. *J. Colloid Interface Sci.* **1977**, *61*, 249.
(65) Pashley, R. M. *J. Colloid Interface Sci.* **1981**, *80*, 153.
(66) Pashley, R. M. *J. Colloid Interface Sci.* **1981**, *83*, 531.
(67) Israelachvili, J. N. *Adv. Colloid Interface Sci.* **1982**, *16*, 31.
(68) Pashley, R. M.; Israelachvili, J. N. *J. Colloid Interface Sci.* **1984**, *97*, 446.
(69) Horn, R. G.; Clarke, D. R.; Clarkson, M. T. *J. Mater. Res.* **1988**, *3*, 413.
(70) Horn, R. G.; Smith, D. T.; Haller, W. *Chem. Phys. Lett.* **1989**, *162*, 404.
(71) Pashley, R. M.; Israelachvili, J. N. *Colloids Surf.* **1981**, *2*, 169.
(72) Marra, J.; Israelachvili, J. N. *Biochemistry* **1985**, *24*, 4608.
(73) Marra, J. *Biophys. J.* **1986**, *50*, 815.
(74) Marra, J. *J. Phys. Chem.* **1986**, *90*, 2145.
(75) Christenson, H. K.; Horn, R. G. *Chem. Phys. Lett.* **1983**, *98*, 45.
(76) Christenson, H. K.; Horn, R. G. *Chem. Scr.* **1985**, *25*, 37.
(77) Abbott, A.; Rutter, P. R.; Berkeley, R. C. W. *J. Gen. Microbiol.* **1983**, *129*, 439.
(78) van Loosdrecht, M. C. M.; Lyklema, J.; Norde, W.; Zehnder, A. J. B. *Microb. Ecol.* **1989**, *17*, 1.
(79) Marshall, K. C.; Stout, R.; Mitchell, R. *J. Gen. Microbiol.* **1971**, *68*, 337.
(80) Huysman, F.; Verstraete, W. *Biol. Fertil. Soils* **1993**, *16*, 21.

(81) Gordon, A. S.; Millero, F. J. *Appl. Environ. Microbiol.* **1984**, *47*, 495.
(82) Davis, P. J. In *Handbook of Mathematical Functions*, Abramowitz, M., Stegun, I. A., Eds.; National Bureau of Standards: Washington, DC, 1964; pp 253−293.
(83) Hogg, R.; Healy, T. W.; Fuerstenau, D. W. *Trans. Faraday Soc.* **1966**, *62*, 1638.
(84) Nir, *S. Prog. Surf. Sci.* **1976**, *8*, 1.

Received for review August 8, 1997. Revised manuscript received February 10, 1998. Accepted February 20, 1998.

ES9707116